Science of the Total Environment 656 (2019) 270–279

Contents lists available at ScienceDirect

Science of the Total Environment

journal homepage: www.elsevier.com/locate/scitotenv

The influence of incorporating microbial fuel cells on greenhouse gas emissions from constructed wetlands

Xiaoou Wang [a], Yimei Tian [a], Hong Liu [b], Xinhua Zhao [a], Sen Peng [a,*]

[a] School of Environmental Science and Engineering, Tianjin University, Tianjin 300350, China
[b] Department of Biological & Ecological Engineering, Oregon State University, 116 Gilmore Hall, Corvallis, OR 97331-3906, USA

HIGHLIGHTS

- Incorporating the MFC significantly reduced the CH_4 and N_2O emissions from CWs.
- CH_4 and N_2O emissions from CW–MFCs increased as external resistance increased.
- CO_2 and CH_4 emissions from CW–MFCs were positively related to organic loadings.
- N_2O emission from CW–MFCs was negatively related to organic loadings.
- Greenhouse gas emissions from CW–MFCs showed significant seasonal variations.

GRAPHICAL ABSTRACT

Integrated constructed wetland–microbial fuel cell (CW–MFC) system:

1. Incorporating the MFC significantly reduced the GHG emissions (by 5.9%–32.4% CO_2 equivalents) from CWs by reducing 17.9%–36.9% CH_4 and 7.2%–38.7% N_2O emissions.
2. CH_4 and N_2O emissions from CW–MFCs significantly increased with increasing external resistance (above 500 Ω), while the CO_2 emission showed the opposite trend.
3. CO_2 and CH_4 emissions from CW–MFCs were positively related to organic loadings.
4. N_2O emission from CW–MFCs was negatively related to organic loadings.
5. Greenhouse gas emissions from CW–MFCs showed significant seasonal variations.

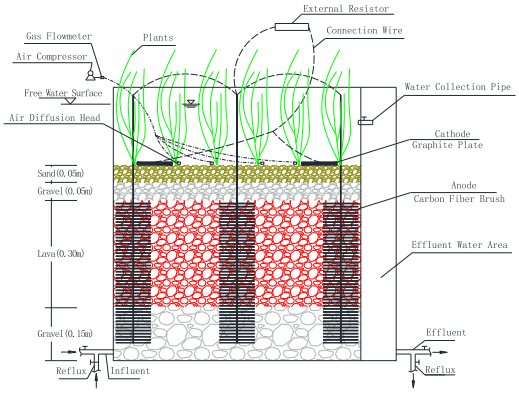

ARTICLE INFO

Article history:
Received 22 August 2018
Received in revised form 14 November 2018
Accepted 21 November 2018
Available online 27 November 2018

Editor: Jose Julio Ortega-Calvo

Keywords:
Constructed wetland
Microbial fuel cell
Greenhouse gases

ABSTRACT

Microbial fuel cells (MFCs) were incorporated into constructed wetlands (CWs) in recent years aiming to enhance the wastewater treatment of CWs while simultaneously produce electricity. However, currently no information is available about the greenhouse gas (GHG) emissions from integrated CW–MFC systems during wastewater treatment. Therefore, this study investigated the influence of incorporating MFCs on GHG (especially CH_4 and N_2O) emissions from CWs under different external resistances, influent organic loadings and seasons. Results showed that incorporating the MFC significantly reduced the GHG emissions (by 5.9%–32.4% CO_2 equivalents) from CWs by reducing 17.9%–36.9% CH_4 and 7.2%–38.7% N_2O emissions. The CH_4 and N_2O emissions from CW–MFCs significantly increased with increasing external resistance (above 500 Ω), while the CO_2 emission showed the opposite trend. However, the CH_4 and N_2O emissions at external resistances below 500 Ω did not differ significantly. There was a significant positive correlation between the CO_2 and CH_4 emissions and influent organic loadings in CW–MFCs, but a significant negative correlation between the N_2O emission and influent organic

* Corresponding author.
E-mail addresses: pengsen_tju@126.com, pengsen@tju.edu.cn (S. Peng).

https://doi.org/10.1016/j.scitotenv.2018.11.328

External resistance
Influent organic loadings

loadings. Influent chemical oxygen demand/total nitrogen (COD/TN) = 3 could result in a TN removal of ≥90% as well as the minimum CO_2 equivalents emission in CW-MFCs. The GHG emissions from CW–MFCs showed significant seasonal variations.

1. Introduction

As a compelling ecological restoration technology, constructed wetlands (CWs) have been widely applied to treat various wastewaters in many countries and regions (Babatunde et al., 2008; Vymazal, 2014; Vymazal and Březinová, 2015; Wu et al., 2011; Zhang et al., 2009; Zhang et al., 2014). However, CWs for wastewater treatment have been found to be sources of greenhouse gases (GHG) (Mander et al., 2014). Carbon dioxide (CO_2) emitted from CWs is generated by aerobic and anaerobic degradation of organic matter by microorganisms, methane (CH_4) is generated by anaerobic degradation of organic matter by methanogens (Sha et al., 2011), and nitrous oxide (N_2O) is produced during nitrification (stepwise conversion of ammonia to nitrate) and denitrification (stepwise conversion of nitrate to nitrogen gas) (Colliver and Stephenson, 2000; Mander et al., 2014; Wunderlin et al., 2013). Although the total GHG emissions from worldwide CWs are currently lower compared with that from all other sources (e.g., natural wetlands, agricultural soil, industry) (Yan et al., 2012), understanding their potential impact on GHG emissions is important due to the continue spread of CWs worldwide.

The GHG emissions from CWs are influenced by several factors including the type and age of CWs, wastewater composition and organic loading, influent feeding mode (batch or continuous), dissolved oxygen (DO), and temperature (Mander et al., 2014; Maucieria et al., 2017). The GHG emissions from different CWs (even from the same CW) therefore greatly fluctuate under different operating conditions. Mander et al. (2014) analyzed 158 papers published from 1994 to 2013 and found that the median values of GHG emissions from different types of CWs were 8.43–12.06 $g/m^2 \cdot d$ for CO_2, 96.0–204.8 $mg/m^2 \cdot d$ for CH_4 and 3.39–4.90 $mg/m^2 \cdot d$ for N_2O. Although CH_4 and N_2O emissions from CWs are much less than the CO_2 emission, CH_4 in the atmosphere has a lifetime of 12.4 years on a 100-year time horizon and a global warming potential of 28 relative to CO_2, while N_2O has an atmospheric lifetime of 121.0 years and a global warming potential of 265 relative to CO_2 over a 100-year time horizon (IPCC, 2013). Therefore, an in-depth understanding of the production and emission of CH_4 and N_2O is of great significance for reducing the GHG emissions from CWs. Mander et al. (2014) reported that hybrid CWs (e.g., the combination of vertical subsurface flow (VSSF), horizontal subsurface flow (HSSF), and free water surface (FWS) CWs) are beneficial for both improvement of water treatment and minimization of GHG emissions, similarly, intermittent loading in VSSF CWs and macrophyte harvesting in HSSF and FWS CWs can mitigate GHG emissions. Pangala et al. (2010) investigated the effect of addition of two potential inhibitors of methanogenesis (iron ochre and gypsum) on net CH_4 emissions in a CW treating farm runoff, and found that ochre addition suppressed CH_4 emissions by 64 ± 13% in the field plot and >90% in laboratory incubations compared to controls. Arends et al. (2014) introduced the anode of a microbial fuel cell (MFC) in the rhizosphere of rice plants, and observed methane emission mitigation in plant-sediment MFC rhizosphere/anode environments.

An MFC typically consists of an anode, cathode, and/or separator. The anode and cathode of the MFC are required to remain anaerobic and aerobic, respectively (Logan, 2008). The organic matter is oxidized by electrogens on the anode, which produces electrons that are transferred to an anode and then flow to a cathode via an external circuit (Doherty et al., 2015; Puig et al., 2012). The protons released during the oxidation of organic matter at the anode travel to the cathode via the bulk fluid (wastewater) or through the separator (Doherty et al., 2015; Puig et al., 2012). The circuit is complete when the electrons and protons are used in a reduction reaction at the cathode with the final electron acceptor normally being oxygen because of its availability and high redox potential (Logan, 2008). Because CWs consist of aerobic and anaerobic zones in which oxidation and reduction processes take place, the redox gradient required for MFC operations can be found naturally in CWs (Doherty et al., 2015). Therefore, MFCs were incorporated into CWs in recent years aiming to enhance the wastewater treatment of CWs while simultaneously produce electricity (Doherty et al., 2015; Xu et al., 2018; Yadav, 2010; Yadav et al., 2012). The successful enhancement of organics and nitrogen removal in CW–MFCs were reported by several studies. For example, Fang et al. (2013) reported that incorporating MFC increased the decolorization rate and chemical oxygen demand (COD_{Cr}) removal rate of the CW by 15% and 12.7%, respectively. Srivastava et al. (2015) reported that the closed-circuit CW–MFCs have performed 27%–49% better than a CW for COD_{Cr} removal. Xu et al. (2018) found that the integration of MFC in CW increased both the nitrification and denitrification rate by approximately 82% in a three-biocathode CW–MFC system. Wang et al. (2016) reported that the relative abundance of beta-*Proteobacteria*, nitrobacteria, and denitrifying bacteria was significantly promoted in a closed-circuit CW–MFC and that the removal rates of nitrate (NO_3^--N) and COD_{Cr} in the CW were improved by an average of 40.2% and 8.3%, respectively.

However, currently no information is available about the GHG emissions from integrated CW–MFC systems during wastewater treatment. Therefore, this study investigated the influence of incorporating MFCs on GHG (especially CH_4 and N_2O) emissions from CWs. The specific objectives of this study were to (Arends et al., 2014) investigate the effects of external resistance and influent organic loadings on GHG emissions from CW–MFCs, and (Babatunde et al., 2008) investigate the seasonal variations of GHG emissions from CW–MFCs.

2. Materials and methods

2.1. Experimental setup

The schematic diagram of four parallel upflow CW–MFC systems (i.e., CW–MFC1, CW–MFC2, CW–MFC3, and CW–MFC4) is shown in Fig. 1. The wetland microcosms were made of Perspex glass with a length of 0.7 m, width of 0.6 m, and height of 1.0 m. The substrates in the microcosms included 20 to 40 mm (equivalent diameter) gravel at the bottom (0.15 m deep), 10 to 30 mm (equivalent diameter) lava as the main substrate layer (0.30 m deep), 5 to 10 mm (equivalent diameter) gravel (0.05 m deep), and 1 to 3 mm (equivalent diameter) sand (0.05 m deep) on the top. A 20% volume of granular graphite with the same particle size as each layer was added to the substrates to increase the conductivity. The pack porosity of the substrates was 0.48. The systems had an approximately 0.20 m deep, free water surface. The effluents were collected with a water collection pipe 0.15 m above the substrate surface and were discharged to the effluent water area (0.1 m long, 0.6 m wide, and 1.0 m high).

Carbon fiber brushes and graphite plates were used as the anode and cathode, respectively. Five carbon fiber brushes were vertically positioned in the middle and at the four corners of the substrates, respectively, and were connected with titanium wires to form a whole anode. The distance between the bottom of the carbon fiber brush and bottom of the substrates was 0.05 m. Each carbon fiber brush (0.7 m long, 0.1 m wide) was made of carbon fiber and titanium wire (diameter of 1 mm); the part containing carbon fiber was 0.4 m long. Four graphite plates (100 × 100 × 8 mm) were evenly placed on the surface of the

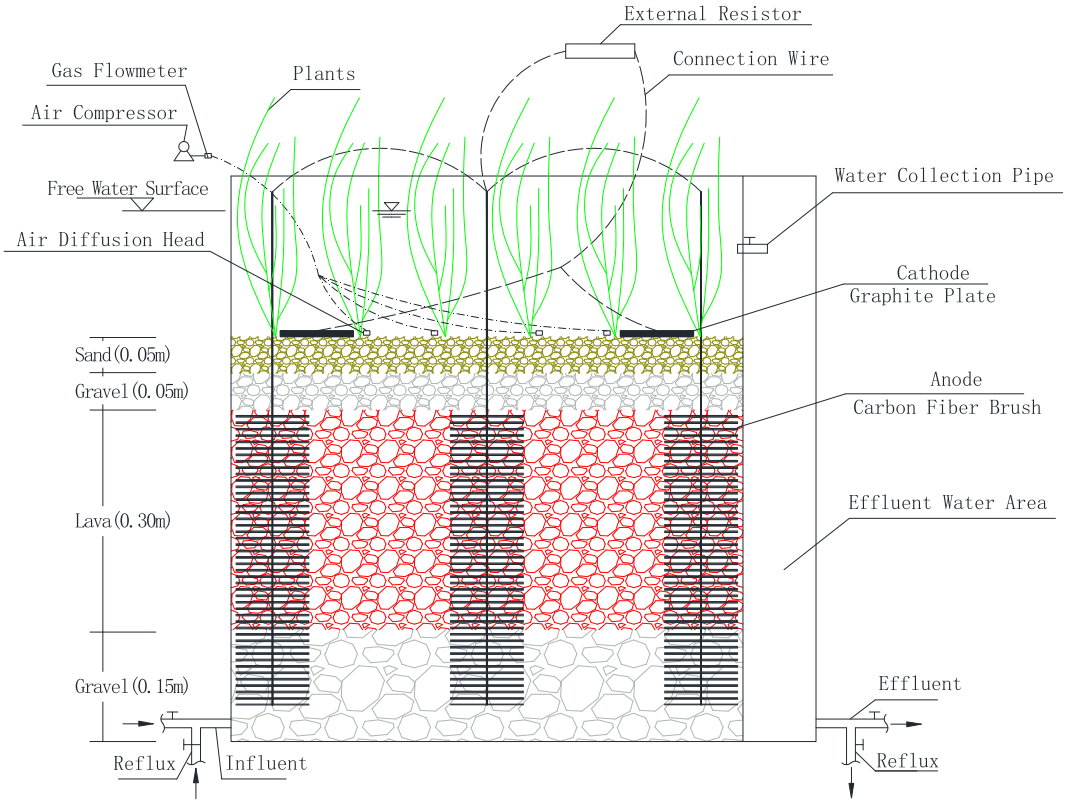

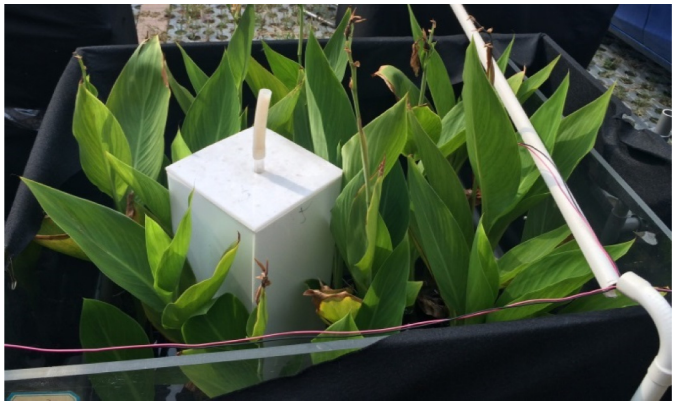

Fig. 1. Schematic diagram of the integrated constructed wetland–microbial fuel cell (CW–MFC) system (above) and the gas sampler in the CW–MFC system (below).

substrate and were connected to each other with titanium wires piercing through the central hole to form a whole cathode. The anode and the cathode were connected with insulated copper wire across an adjustable external resistor (0–9999.9 Ω). Before use, the graphite plate was immersed in 1 mol/L HCL solution for 2 h to remove impurity ions, then rinsed with deionized water, and dried.

Canna indica was selected and planted in the wetland microcosms. The microcosms were submerged in tap water immediately after planting to allow the development of plants and microbes. 15 NH_4Cl, 15 KH_2PO_4, 15 $MgSO_4 \cdot 7H_2O$, and 15 $CaCl_2 \cdot 2H_2O$ (in mg/1 L tap water) were added to the tap water to enhance the growth of plants. After one month, the MFC circuit was connected and the external resistors were set to 1000 Ω to start up the four CW–MFC systems.

During the system startup, the mixture of an aerobic sludge and an anaerobic sludge supernatant (1:1 ratio) collected from the Jingu Municipal Wastewater Treatment Plant (Tianjin, China) was used as inoculum and sodium acetate was used as carbon source. The supernatant and sodium acetate solution (500 mg/L) were mixed (1:1 ratio) and the mixed solution was continuously pumped into the systems at a flow rate of 0.073 m^3/d with a hydraulic retention time (HRT) of 1.5 d. To enhance the development of microbes on the cathodes, graphite plates were inoculated in the mixed solution for 24 h before the startup of the CW–MFCs, and were then placed in the cathode area. To accelerate the enrichment of electrogens on the anodes, 50% of the effluent was returned to the systems. After 10 d of operation, reproducible maximum voltages (0.73–0.74 V) were observed in the four CW–MFCs, indicating the successful startup of the systems.

After successful startup, the influents were continuously pumped into the systems to start the experiment. The average HRT in the systems was 1.5 d. The DO concentration in the cathode area was maintained at 1.5 mg/L by continuous aeration. The aeration intensity was controlled with gas flowmeters connected to an air compressor. 50% of the effluent was returned to the systems to enhance the pollutant removal. After 7–8 d of operation, the output voltage of the CW–MFC systems stabilized, and samples were taken and then analyzed.

The influent was a synthetic domestic wastewater and was prepared using the following chemicals: CH_3COONa, $C_2H_5NO_2$, NH_4Cl, $NaNO_2$, KNO_3, $Na_5P_3O_{10}$, KH_2PO_4, $CaCl_2 \cdot 2H_2O$, and $MgSO_4 \cdot 7H_2O$. All chemicals

were of analytical grade. The major characteristics of the influents were pH 7.0 ± 0.10, 15 mg/L organic nitrogen, 25 mg/L ammonia nitrogen (NH_3-N), 0.1 mg/L nitrite (NO_2^--N), 0.5 mg/L NO_3^--N, 40.6 mg/L total nitrogen (TN), 1 mg/L tripolyphosphate ($P_3O_{10}^{5-}$-P), 4 mg/L phosphate (PO_4^{3-}-P), and 5 mg/L total phosphorus (TP). The influent COD_{Cr} concentrations selected for this study were 50 mg/L, 80 mg/L, 120 mg/L, 200 mg/L, 280 mg/L, and 360 mg/L and the corresponding influent C/N ratios were 1.23, 2, 3, 5, 7, and 9, respectively.

2.2. Sampling and analysis

The closed-chamber method (Mander et al., 2003, 2015) was used to measure the CO_2, CH_4, and N_2O emissions. One gas sampler (length, width, and height of 0.15 × 0.15 × 0.50 m) was inserted 0.10 m into the substrate in each CW–MFC system (Fig. 1). The gas sampler was made of nontransparent white polypropylene (PP) with a hole (1 cm diameter) on the top and a hole (0.10 m diameter) at the bottom. A 0.10 m long latex hose was attached to the hole on the top for gas monitoring. The latex hose was open during the operation of the CW–MFCs, and was sealed by a long tail clip and a butyl rubber plug for 24 h during gas sampling. The difference between the two readings before and after the sealing was the gas emission flux (per 24 h) of the CW–MFCs. The concentration of CO_2, CH_4, and N_2O inside the gas sampler was determined with portable high-precision gas detectors with built-in micro-sampling pumps (Model TD1198-CO_2, TD1198-CH_4, and TD1198-N_2O, Beijing Tiandishouhe Technology Development Co., Ltd., China). All readings were carried out from 9 to 10 am to avoid deviations caused by the monitoring time.

Water samples were collected every 3 d, and were analyzed immediately in the laboratory for COD_{Cr} and TN using a Digital Reactor Block 200 and a HACH DR 2800 spectrophotometer, according to the standard methods provided by HACH Company, USA. The wastewater DO within the CW–MFC systems was measured every 30 min using an online DO detector (Model SIN-DM2800, Hangzhou Sinomeasure Automation Technology Co., Ltd., China). The output voltage (U) was measured with a multi-channel data logger (Model CT-4008-5v10mA-164, Shenzhen Neware Electronics Co., Ltd., China) and data were collected at intervals of 30 min. The ambient temperature was monitored with a temperature recorder (Model TH6, Hangzhou Sinomeasure Automation Technology Co., Ltd., China) and data were collected at intervals of 30 min.

2.3. Data analysis

The mass concentration (mg/m^3) of CO_2 and N_2O was directly recorded by CO_2 and N_2O detectors, respectively. The reading of the CH_4 detector was converted from vol% to ppm (volume concentration) as follows:

$$\text{ppm} = 1\ \text{vol}\% \times 10^{-4} \tag{1}$$

The mass concentration (C, mg/m^3) of CH_4 was obtained by:

$$C = \text{ppm} \times \frac{MP}{RT} \tag{2}$$

where M is the molecular weight of the gas (g/mol), P is the atmospheric pressure in the closed-chamber (Pa), T is the absolute temperature in the closed-chamber (K), R is the gas constant (8.314 J/(mol·K)).

The emission fluxes (J_{GHG}, mg/m^2·d) of CO_2, CH_4, and N_2O were calculated as follows:

$$J_{GHG} = \frac{dc}{dt} \times \frac{V}{A} = \frac{d(\text{ppm})}{dt} \times \frac{V}{A} \times \frac{MP}{RT} \tag{3}$$

where dc/dt is the gas mass concentration change in the closed-chamber per unit time (mg/m^3·d), V is the volume of the gas sampler above the free water surface in the CW–MFC system (0.15 × 0.15 × 0.20 m = 0.0045 m^3 in this study), A is the intake area at the bottom of the gas sampler (π × 0.1^2/4 ≈ 0.007854 m^2 in this study).

The emission flux of CO_2 equivalents (CO_2-eq) was calculated as follows:

$$J_{CO_2-eq} = J_{CO_2} + 28 \times J_{CH_4} + 265 \times J_{N_2O} \tag{4}$$

where J_{CO_2} is the CO_2 emission flux (mg/m^2·d), J_{CH4} is the CH_4 emission flux (mg/m^2·d), J_{N2O} is the N_2O emission flux (mg/m^2·d), "28" is the global warming potential of CH_4 relative to CO_2 (IPCC, 2013), and "265" is the global warming potential of N_2O relative to CO_2 (IPCC, 2013).

The removal rates (R) of COD_{Cr} and TN were calculated as follows:

$$R = \frac{(C_i - C_e)}{C_i} \times 100\% \tag{5}$$

where C_i is the mean influent concentration (mg/L) and C_e is the mean effluent concentration (mg/L).

The current (I) is calculated using Ohm's law:

$$I = \frac{U}{R_{ex}} \tag{6}$$

where U is the output voltage (V) and R_{ex} is the external resistance (Ω).

The power density (P_d) was calculated as follows:

$$P_d = \frac{P}{V} = \frac{U^2}{VR_{ex}} \tag{7}$$

where P is the power, V is the total volume of the CW–MFC (0.23 m^3 in this study), U is the output voltage (V), and R_{ex} is the external resistance (Ω).

To investigate the statistical difference of the GHG emissions under different conditions, tests for significant differences among the CW–MFC systems were performed at the significance level of 0.05 using one-way analysis of variance (ANOVA) followed by a Duncan post hoc test ($p < 0.05$). All statistical analyses were performed with SPSS and Origin software.

3. Results and discussion

3.1. Wastewater DO across the CW–MFC system

Fig. 2 shows the variation in the wastewater DO across the CW–MFCs. Comparing Fig. 2(A) and (B), the wastewater DO concentration distribution in both closed-circuit CW–MFC and open-circuit CW–MFC varied in the same manner. The effluent DO concentration remained at approximately 1.5 mg/L due to artificial aeration. The refluxed effluent introduced a certain amount of DO to the bottom of the CW–MFCs, and the DO concentration at 15 cm from the bottom (0.38–0.49 mg/L) was slightly higher than that in the influent (0.19–0.31 mg/L). As it was continuously consumed along the path of the wastewater, the DO concentration at 30 cm from the bottom decreased to 0.20–0.31 mg/L, while that at 45 cm from the bottom increased to 0.47–0.61 mg/L as it was in close proximity to the substrates' surface.

Overall, the cathode area of CW–MFCs remained under aerobic conditions (DO >1.0 mg/L) due to aeration, while the anode area inside the reactors was dominated by anoxic/anaerobic conditions (DO <0.5 mg/L). This met the redox conditions required by the MFC to function efficiently (Zhao et al., 2013).

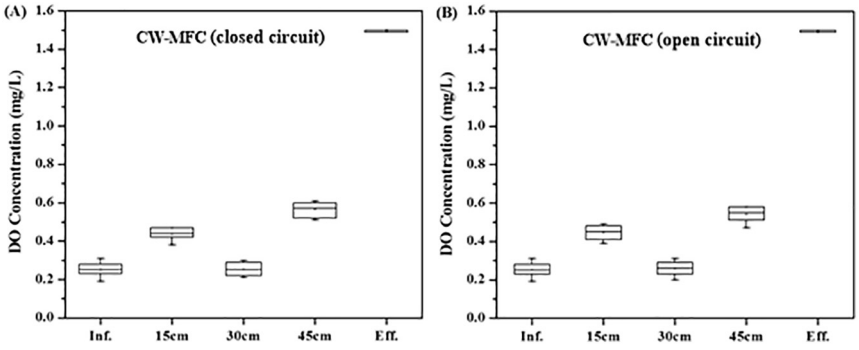

Fig. 2. Wastewater DO profiles across the integrated constructed wetland–microbial fuel cell (CW–MFC) systems.

3.2. Effects of the external resistance on GHG emissions

The experiments in Section 3.1 were carried out from May to September 2016. The recorded daily average minimum and maximum temperatures were 11 °C–27 °C and 18 °C–36 °C, respectively, and the five-day average temperatures varied between 20.3 °C and 30.1 °C. According to the monitoring results, there were no large fluctuations in GHG emissions from CW-MFCs at five-day average temperatures above 18 °C. Therefore, the effect of the temperature on the GHG emissions is not discussed in this section. The influent COD_{Cr} concentration was 200 mg/L and the corresponding C/N ratio was 5. The circuit of CW–MFC1 was connected and the circuit of CW–MFC2 was disconnected as a control. The average emission fluxes of CO_2, CH_4, N_2O, and CO_2-eq, and the corresponding COD_{Cr}, TN removal in the closed-circuit CW–MFC1 under different external resistances and in the open-circuit CW–MFC2 are shown in Fig. 3.

The average GHG emission fluxes from CW–MFC1 under different external resistances (50–2000 Ω) were 2.39–2.74 g $CO_2/m^2 \cdot d$, 78.67–-94.19 mg $CH_4/m^2 \cdot d$, and 2.60–3.33 mg $N_2O/m^2 \cdot d$ and the corresponding CO_2-eq emission was 5.61–5.87 g/$m^2 \cdot d$. Compared with the average GHG emissions from CW–MFC2 (2.37 g $CO_2/m^2 \cdot d$, 114.69 mg $CH_4/m^2 \cdot d$, 3.59 mg $N_2O/m^2 \cdot d$, and 6.53 g CO_2-eq/$m^2 \cdot d$), the CO_2 emission from CW–MFC1 was higher by an average of 0.8%–15.6%, while the CH_4 and N_2O emissions were significantly ($p < 0.05$) lower by an average of 17.9%–31.4% and 7.2%–27.6%, respectively. Because of the lower CH_4 and N_2O emissions, the CO_2-eq emission from CW–MFC1 was significantly ($p < 0.05$) lower than that from CW–MFC2 by an average of 10.1%–14.1%. This demonstrated that the MFC significantly reduced the GHG emissions from CWs by reducing the CH_4 and N_2O emissions.

The ANOVA results showed that, there was no significant ($p > 0.05$) difference in the CH_4 and N_2O emissions from CW–MFC1 when the external resistance was below 500 Ω, and the CO_2 emission from CW–MFC1 varied only between 2.60 and 2.69 g/$m^2 \cdot d$. When the external resistance exceeded 500 Ω, the CH_4 and N_2O emissions from CW–MFC1 significantly ($p < 0.05$) increased with increasing external resistance, while the CO_2 emission from CW–MFC1 significantly ($p < 0.05$) decreased. Because of the opposite trend of the CH_4 and N_2O, and CO_2 emissions, no significant ($p > 0.05$) difference was observed for the CO_2-eq emission from CW–MFC1 when the external resistance was below 1000 Ω.

In an MFC, organic substrates are oxidized by electrogens in the anodic cell, which produces electrons that are transferred to an anode and then flow to a cathode (Puig et al., 2012). The bacteria on the cathode can use the electrons to reduce nitrite and nitrate to N_2 (Puig et al., 2012; Samrat et al., 2018), which can promote the nitrogen removal and reduce the accumulation of N_2O during nitrification and denitrification. This was proved by the higher average TN removal (84.3%–91.4%) in closed-circuit CW-MFC1 than that (80.6%) in open-circuit CW-MFC2 (Fig. 3(F)). MFC can also enhance the anaerobic degradation of organics in the anodes, thus improving the organic removal of CW–MFC systems (Doherty et al., 2015) and increasing the production of CO_2. This was proved by the higher average COD_{Cr} removal (81.4%–91.6%) in closed-circuit CW-MFC1 than that (78.5%) in open-circuit CW-MFC2 (Fig. 3(E)). A higher current indicated a faster degradation of organics by electrogens in the MFC (Liu et al., 2005). Moreover, the electrogens on anodes in the MFC may compete with methanogens for organic substrates and thus reduce the production of CH_4 (Arends et al., 2014). As the external resistance increased, the output current from the CW–MFC decreased (Fig. 6(A)). On one hand, the lower current in an MFC was not in favor of the consumption of organics by electrogens, which can be seen from the decreased COD_{Cr} removal with the increase of external resistance (Fig. 3(E)), and thus the production of CO_2 was reduced. On the other hand, the lower current reduced the competitiveness of electrogens with methanogens on organic substrates, resulting in an increased production of CH_4. Moreover, the decreased current provided less electrons for denitrification in the cathode, leading to the decrease of TN removal (Fig. 3(F)) and the accumulation of N_2O. This explained the increased CH_4 and N_2O emissions and decreased CO_2 emission from CW–MFC1 with increasing external resistance.

3.3. Effects of influent organic loadings on GHG emissions

The experiments in Section 3.2 were carried out from April to August 2017. The recorded daily average minimum and maximum temperatures were 14 °C–28 °C and 20 °C–38 °C, respectively, and the five-day average temperatures varied between 20.2 °C and 31.3 °C. According to the monitoring results, there were no large fluctuations in GHG emissions from CW-MFCs at five-day average temperatures above 18 °C. Therefore, the effect of the temperature on the GHG emissions is not discussed in this section. The external resistance of CW–MFC1 was set to 250 Ω and the circuit of CW–MFC2 was disconnected as a control. The average emission fluxes of CO_2, CH_4, N_2O, and CO_2-eq, and the corresponding COD_{Cr}, TN removal in the closed-circuit CW–MFC1 and open-circuit CW–MFC2 under different influent organic loadings are shown in Fig. 4.

The average GHG emission fluxes from CW–MFC1 under different influent organic loadings (50–360 mg/L COD_{Cr}) were 0.79–4.45 g $CO_2/m^2 \cdot d$, 23.74–144.65 mg $CH_4/m^2 \cdot d$, and 1.72–-11.92 mg $N_2O/m^2 \cdot d$ and the corresponding CO_2-eq emission was 3.99–8.96 g/$m^2 \cdot d$. Compared with the average GHG emissions from CW–MFC2 (0.72–3.85 g $CO_2/m^2 \cdot d$, 33.79–223.94 mg $CH_4/m^2 \cdot d$, 2.11–-19.45 mg $N_2O/m^2 \cdot d$, and 5.30–10.68 g CO_2-eq/$m^2 \cdot d$), the CO_2 emission from CW–MFC1 was significantly ($p < 0.05$) higher by an average of 9.7%–15.6%, while the CH_4 and N_2O emissions were significantly ($p < 0.05$) lower by an average of 29.7%–35.4% and 18.5%–38.7%, respectively. Because of the lower CH_4 and N_2O emissions, the CO_2-eq emission from CW–MFC1 was significantly ($p < 0.05$) reduced by an average of 13.8%–32.4%, compared with that of CW–MFC2. This further demonstrated that the MFC significantly reduced the GHG emissions from CWs, especially the emissions of CH_4 and N_2O. The ANOVA results

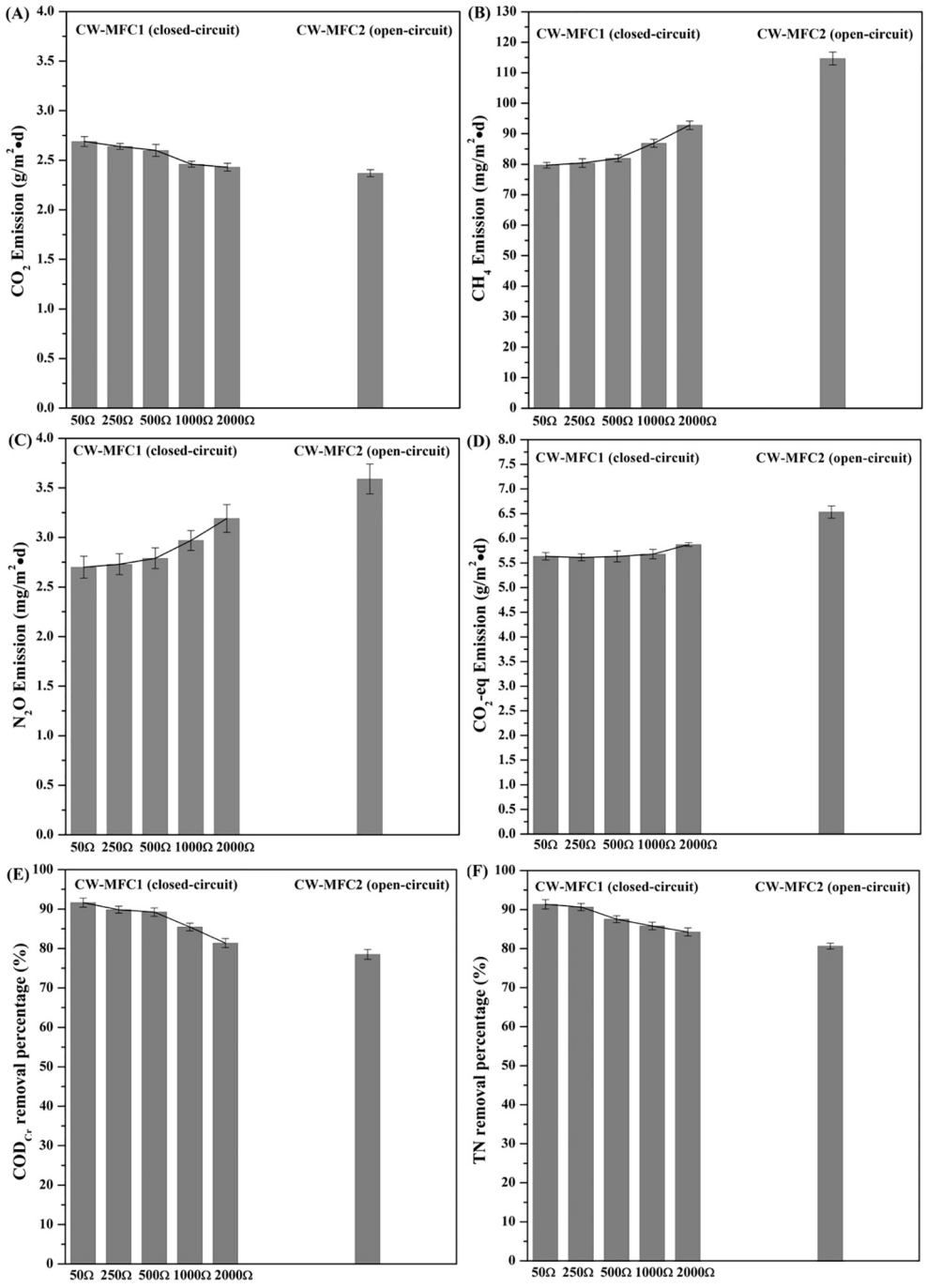

Fig. 3. Emission fluxes of greenhouse gases ((A), (B), (C), (D)) and the corresponding COD_{Cr}, TN removal ((E), (F)) from the integrated constructed wetland–microbial fuel cell (CW–MFC) systems under different external resistances. The error bars represent plus/minus one standard deviation.

showed significant ($p < 0.05$) difference in the CO_2, CH_4 and N_2O emissions from both the CW–MFC1 and CW–MFC2 under different influent organic loadings, demonstrating the significant effect of influent organic loadings on the GHG emissions from CW–MFCs.

As shown in Fig. 4(A) and (B), the CO_2 and CH_4 emissions from CW–MFC1 and CW–MFC2 increased approximately 4.6 and 5.1 times and 4.3 and 5.6 times, respectively, as the influent COD_{Cr} concentrations increased from 50 mg/L to 360 mg/L. The larger the influent organic loading, the greater was the increase of the CO_2 and CH_4 emissions (Fig. 4 (A) and (B)). Many studies showed that the CO_2 and CH_4 emissions from CWs increased with increasing influent organic loadings (Corbella and Puigagut, 2015; Yan et al., 2012). This was mainly because higher organics supported more active microbial activity, resulting in a higher production of CO_2 and consumption of DO. The reduction of DO was conducive to the growth of methanogens, thereby increasing the CH_4 emission. As the influent COD_{Cr} concentrations increased from 50 mg/L to 360 mg/L, the N_2O emission from CW–MFC1 and CW–MFC2 decreased by approximately 85.6% and 89.2%, respectively. The influent organic loadings affected the N_2O emission from CWs mainly by influencing the microbial nitrification and denitrification (Ding et al., 2012; Wu et al., 2009). When the influent organic loadings increased, more organic carbons are available for denitrifying bacteria and also increase the metabolism of electrogens and improve the electricity output of MFCs (Martin et al., 2010; Velvizhi and Mohan, 2012). This was proved by the increased voltage, current and power density from CW–MFC1 with increasing influent organic loadings (Fig. 6(B)).

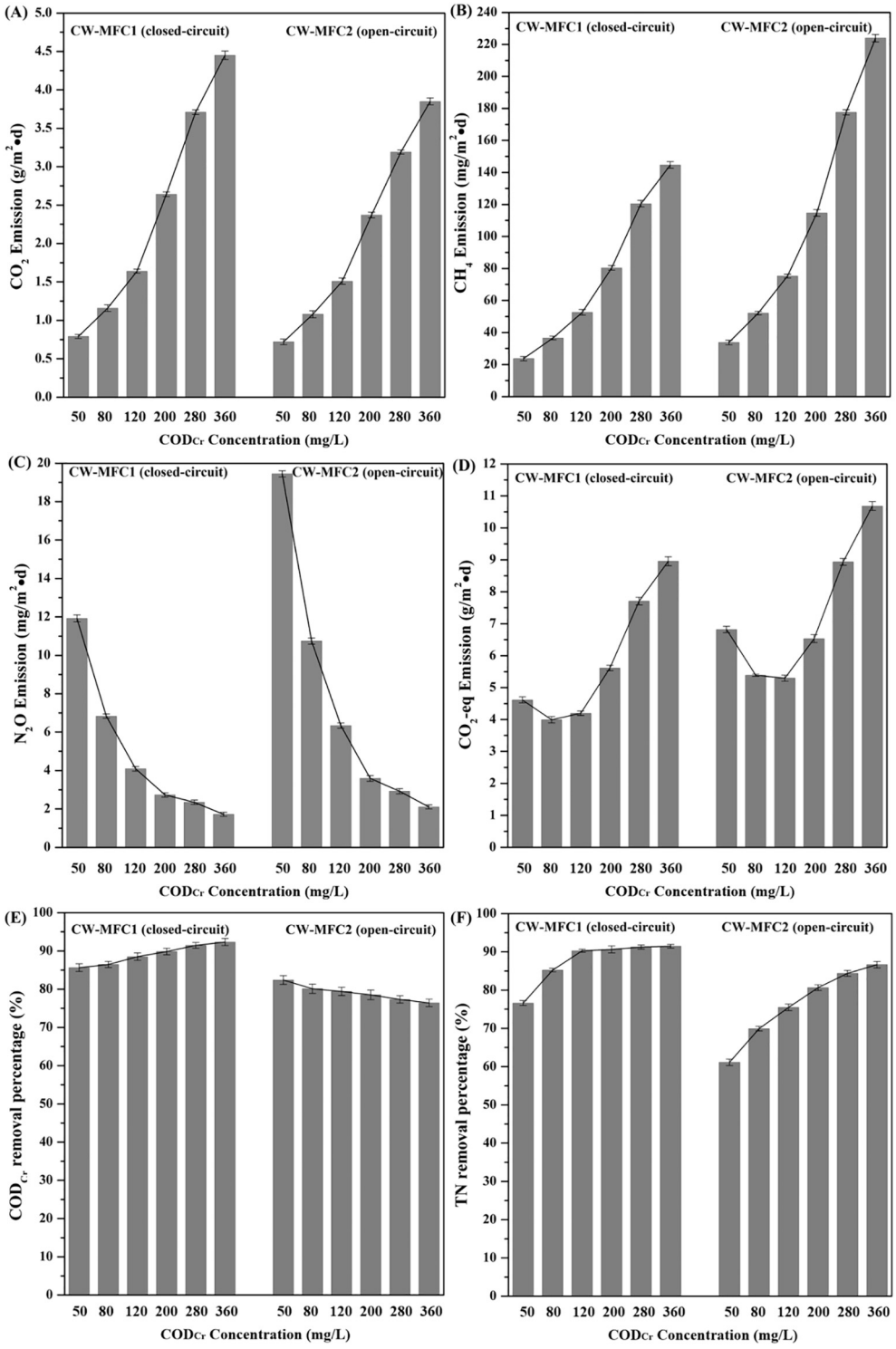

Fig. 4. Emission fluxes of greenhouse gases ((A), (B), (C), (D)) and the corresponding COD_{Cr}, TN removal ((E), (F)) from the integrated constructed wetland–microbial fuel cell (CW–MFC) systems under different influent organic loadings. The error bars represent plus/minus one standard deviation.

The increased current provided more electrons for denitrification on cathode, leading to more thorough denitrification and the increase of TN removal (Fig. 4(F)), and thus the accumulation and emission of N_2O reduced. Moreover, the increased current was beneficial to the consumption of organics by electrogens, which was proved by the increased COD_{Cr} removal from closed-circuit CW-MFC1 with increasing influent organic loadings (Fig. 4(E)). The increase of TN removal and decrease of the N_2O emission with increasing influent organic loadings notably slowed down when the influent COD_{Cr} concentrations exceeded 120 mg/L in the closed-circuit CW–MFC1 and exceeded 200 mg/L in the open-circuit CW–MFC2 (Fig. 4(C) and (F)). Together with the lower N_2O emission and higher TN removal (Fig. 4(F)) from CW–MFC1, this indicated that the MFC led to a more thorough denitrification process in CWs, especially at lower influent organic loadings. Because of the opposite trend of the CO_2 and CH_4 emissions and N_2O emission the minimum CO_2-eq emission was achieved at influent organic loadings of 80–120 mg/L COD_{Cr} in both the CW–MFC1 and CW–MFC2 (Fig. 4(D)). Moreover, it was concluded that influent COD/TN = 3 could result in

a TN removal of ≥90% as well as the minimum CO_2-eq emission in CW-MFCs.

Overall, the influent organic loadings significantly influenced the GHG emissions from CW–MFC systems. There was a significant ($p < 0.05$) positive correlation between the CO_2 and CH_4 emissions and influent organic loadings, while a significant ($p < 0.05$) negative correlation was observed between the N_2O emission and influent organic loadings.

3.4. Seasonal variations of GHG emissions

The experiments in Section 3.3 were carried out from September 2016 to August 2017. The operation of the systems was stopped during the winter icing period (December 13, 2016, to February 13, 2017). The experimental period covered the four seasons of autumn (five-day average temperature of 22 °C–10 °C), winter (five-day average temperature < 10 °C), spring (five-day average temperature of 10 °C–22 °C), and summer (five-day average temperature > 22 °C). The influent COD_{Cr} concentration was 200 mg/L and the corresponding C/N ratio was 5. The external resistance of CW–MFC3 was set to 250 Ω and the circuit of CW–MFC4 was disconnected as a control. The emission fluxes of CO_2, CH_4, N_2O, and CO_2-eq, and the corresponding COD_{Cr}, TN removal from the closed-circuit CW–MFC3 and open-circuit CW–MFC4 during different seasons are shown in Fig. 5.

Compared with the GHG emissions from CW–MFC4 during the four seasons, the CO_2 emission from CW–MFC3 was significantly ($p < 0.05$) higher by an average of 10.2%–42.4%, while the CH_4 and N_2O emissions were significantly ($p < 0.05$) lower by an average of 21.9%–36.9% and 19.1%–26.6%, respectively, which contributed to lower CO_2-eq emission from CW–MFC3 by an average of 5.9%–15.4%. During summer, autumn and winter, the CO_2-eq emission from CW–MFC3 was significantly ($p < 0.05$) lower than that from CW–MFC4 by an average of 13.0%–15.4%, while there was no significant ($p > 0.05$) difference in the CO_2-eq emission between CW–MFC3 and CW–MFC4 during spring. According to the ANOVA results, For both CW–MFC3 and CW–MFC4, (Arends et al., 2014) there was no significant ($p > 0.05$) difference in the GHG emissions between summer and autumn, and (Babatunde et al., 2008) the GHG emissions during summer and autumn were significantly ($p < 0.05$) higher than that during spring, which are significantly ($p < 0.05$) higher than that during winter. The average emissions of CO_2, CH_4, N_2O, and CO_2-eq from CW–MFC3 during summer were 2.2 times, 1.7 times, 2.2 times and 1.7 times higher than that during winter, respectively. From the analysis of Fig. 5(A), (B), (C) and (D) in conjunction with Fig. 5 (E) and (F), it can be seen that the seasonal variation trend of GHG emissions from CW–MFCs were consistent with that of COD_{Cr} and TN removal.

The seasonal variations of the GHG emissions from CW–MFCs in this study were consistent with the findings of many studies on GHG emissions from CWs. For example, Wu et al. (2016) observed a notable seasonal variability of the average CO_2 fluxes (ranging from −14.23 to 13.29 $g/m^2 \cdot d$) from a FWS CW and the CO_2 emission during summer was the highest. Søvik et al. (2006) reported that the N_2O and CH_4 emissions from CWs were significantly higher during summer than during winter. Teiter and Mander (2005) observed a significantly higher release of N_2O, CH_4, and CO_2 from CWs during the warmer period. Bateganya et al. (2015) obtained a significant ($p < 0.05$) positive correlation between the temperature and all gaseous fluxes (CO_2, N_2O, and CH_4) from subsurface-flow CWs. The ambient temperature influenced the GHG emissions from CWs primarily by affecting the microbial activity. At lower temperatures, the activity of microorganisms, including methanogens and nitrifying and denitrifying bacteria was relatively

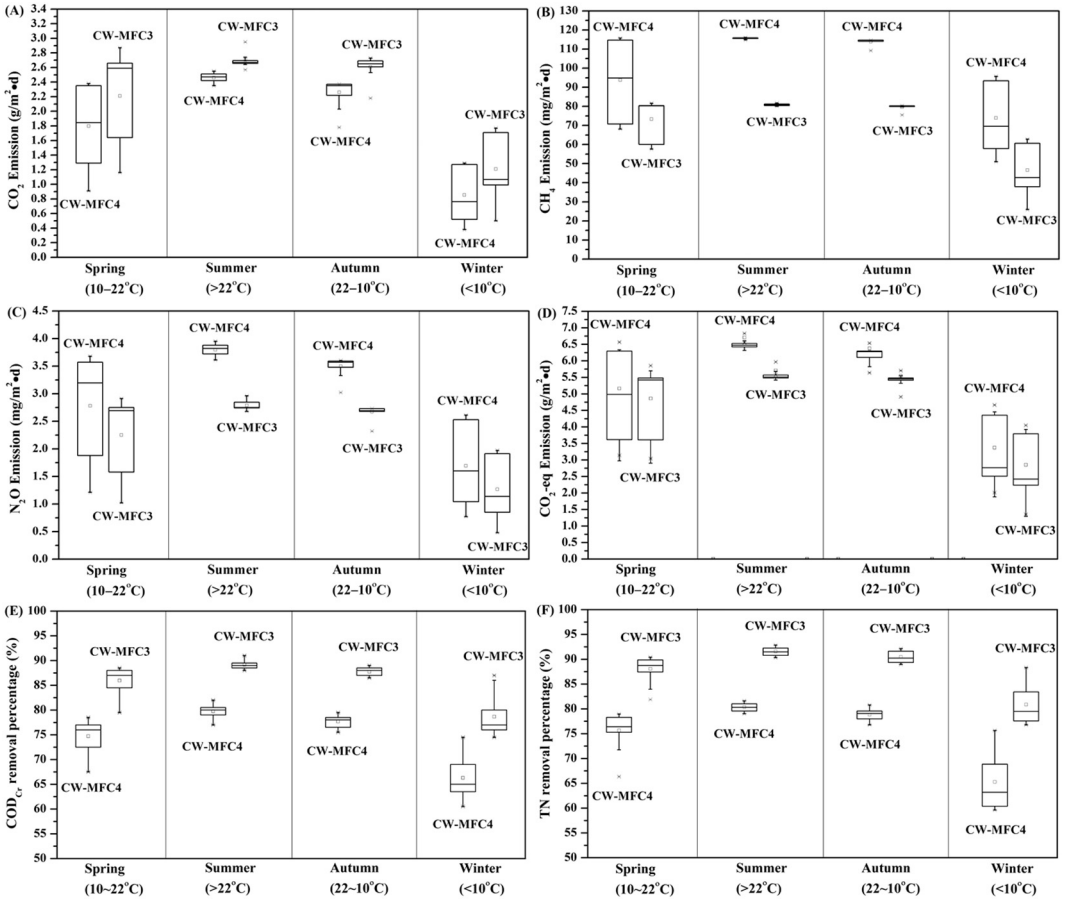

Fig. 5. Emission fluxes of greenhouse gases ((A), (B), (C), (D)) and the corresponding COD_{Cr}, TN removal ((E), (F)) from the integrated constructed wetland–microbial fuel cell (CW–MFC) systems (closed-circuit CW–MFC3 and open-circuit CW–MFC4) during different seasons.

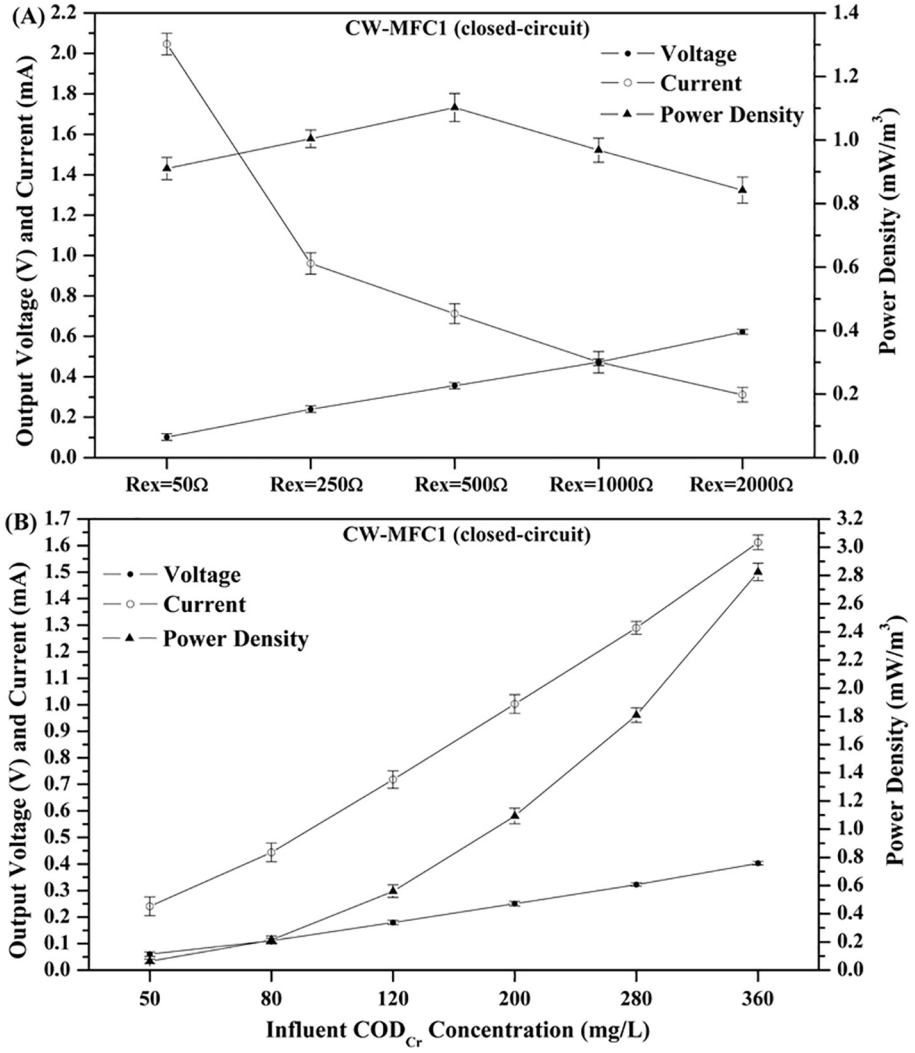

Fig. 6. Average output voltage, current and power density of the integrated constructed wetland–microbial fuel cell (CW–MFC) system under different external resistances (A) and influent organic loadings (B). The error bars represent plus/minus one standard deviation.

weak (Søvik et al., 2006; Wu et al., 2016); therefore the removal of COD_{Cr} and TN was reduced (Fig. 5(E) and (F)), and the generation of CO_2, CH_4, and N_2O was also reduced.

Overall, GHG emissions from the CW–MFC were significantly influenced by the ambient temperature, which showed significant seasonal variations. The MFC significantly reduced the CH_4 and N_2O emissions during each season and thus reduced the CO_2-eq emission from the CW.

4. Conclusions

Incorporating the MFC significantly reduced the GHG emissions (by 5.9%–32.4% CO_2 equivalents) from CWs by reducing 17.9%–36.9% CH_4 and 7.2%–38.7% N_2O emissions. The CH_4 and N_2O emissions from CW–MFCs significantly increased with increasing external resistance (above 500 Ω), while the CO_2 emission showed the opposite trend. However, the CH_4 and N_2O emissions at external resistances below 500 Ω did not differ significantly. There was a significant positive correlation between the CO_2 and CH_4 emissions and influent organic loadings in CW–MFCs, but a significant negative correlation between the N_2O emission and influent organic loadings. Influent COD/TN = 3 could result in a TN removal of ≥90% as well as the minimum CO_2 equivalents emission in CW-MFCs. The GHG emissions from CW–MFCs showed significant seasonal variations.

Acknowledgments

This research was supported by The Key Special Program on the S&T for the Pollution Control and Treatment of Water Bodies of China (2014ZX07203-009). Xiaoou Wang is grateful for the financial support from China Scholarship Council (No. 201706250159).

Appendix A. Supplementary data

Supplementary data to this article can be found online at https://doi.org/10.1016/j.scitotenv.2018.11.328.

References

Arends, J.B.A., Speeckaert, J., Blondeel, E., Vrieze, J.D., Boeckx, P., Verstraete, W., Rabaey, K., Boon, N., 2014. Greenhouse gas emissions from rice microcosms amended with a plant microbial fuel cell. Appl. Microbiol. Biotechnol. 98 (7), 3205–3217.

Babatunde, A.O., Zhao, Y.Q., O'Neill, M., O'Sullivan, B., 2008. Constructed wetlands for environmental pollution control: a review of developments, research and practice in Ireland. Environ. Int. 34, 116–126.

Bateganya, N.L., Mentler, A., Langergraber, G., Busulwa, H., Hein, T., 2015. Carbon and nitrogen gaseous fluxes from subsurface flow wetland buffer strips at mesocosm scale in East Africa. Ecol. Eng. 85, 173–184.

Colliver, B.B., Stephenson, T., 2000. Production of nitrogen oxide and dinitrogen oxide by autotrophic nitrifiers. Biotechnol. Adv. 18 (3), 219–232.

Corbella, C., Puigagut, J., 2015. Effect of primary treatment and organic loading on methane emissions from horizontal subsurface flow constructed wetlands treating urban wastewater. Ecol. Eng. 80, 79–84.

Ding, Y., Song, X.S., Wang, Y.H., Yan, D.H., 2012. Effects of dissolved oxygen and influent COD/N ratios on nitrogen removal in horizontal subsurface flow constructed wetland. Ecol. Eng. 46, 107–111.
Doherty, L., Zhao, Y.Q., Zhao, X.H., Hu, Y.S., Hao, X.D., Xu, L., Liu, R.B., 2015. A review of a recently emerged technology: constructed wetland-microbial fuel cells. Water Res. 85, 38–45.
Fang, Z., Song, H.L., Cang, N., Li, X.N., 2013. Performance of microbial fuel cell coupled constructed wetland system for decolorization of azo dye and bioelectricity generation. Bioresour. Technol. 144, 165–171.
IPCC, 2013. Climate Change: The Physical Science Basis. Cambridge University Press, Cambridge.
Liu, H., Cheng, S., Logan, B.E., 2005. Power generation in fed-batch microbial fuel cells as a function of ionic strength, temperature, and reactor configuration. Environ. Sci. Technol. 39 (14), 5488–5493.
Logan, B.E., 2008. Microbial Fuel Cells. John Wiley and Sons, Inc., Hoboken, New Jersey.
Mander, Ü., Kuusemets, V., Lõhmus, K., Mauring, T., Teiter, S., Augustin, J., 2003. Nitrous oxide dinitrogen, and methane emission in a subsurface flow constructed wetland. Water Sci. Technol. 48, 135–142.
Mander, Ü., Dotro, G., Ebie, Y., Towprayoon, S., Chiemchaisri, C., Nogueira, S.F., Jamsranjav, B., Kasak, K., Truu, J., Tournebize, J., Mitsch, W.J., 2014. Greenhouse gas emission in constructed wetlands for wastewater treatment: a review. Ecol. Eng. 66, 19–35.
Mander, Ü., Maddison, M., Soosaar, K., Koger, H., Teemusk, A., Truu, J., Well, R., Sebilo, M., 2015. The impact of a pulsing water table on wastewater purification and greenhouse gas emission in a horizontal subsurface flow constructed wetland. Ecol. Eng. 80, 69–78.
Martin, E., Savadogo, O., Guiot, S.R., Tartakovsky, B., 2010. The influence of operational conditions on the performance of a microbial fuel cell seeded with mesophilic anaerobic sludge. Biochem. Eng. J. 51 (3), 132–139.
Maucieria, C., Barbera, A.C., Vymazal, J., Borin, M., 2017. A review on the main affecting factors of greenhouse gases emission in constructed wetlands. Agric. For. Meteorol. 236, 175–193.
Pangala, S.R., Reay, D.S., Heal, K.V., 2010. Mitigation of methane emissions from constructed farm wetlands. Chemosphere 78 (5), 493–499.
Puig, S., Coma, M., Desloover, J., Boon, N., Colprim, J., Balaguer, M.D., 2012. Autotrophic denitrification in microbial fuel cells treating low ionic strength waters. Environ. Sci. Technol. 46 (4), 2309–2315.
Samrat, M.V.V.N., Rao, K.K., Ruggeri, B., Tommasi, T., 2018. Denitrification of water in a microbial fuel cell (MFC) using seawater bacteria. J. Clean. Prod. 178, 449–456.
Sha, C.Y., Mitsch, W.J., Mander, Ü., Lu, J., Batson, J., Zhang, L., He, W.S., 2011. Methane emissions from freshwater riverine wetlands. Ecol. Eng. 37 (1), 16–24.
Søvik, A.K., Augustin, J., Heikkinen, K., Huttunen, J.T., Necki, J.M., Karjalainen, S.M., Kløve, B., Liikanen, A., Mander, Ü., Puustinen, M., Teiter, S., Wachniew, P., 2006. Emission of the greenhouse gases nitrous oxide and methane from constructed wetlands in Europe. J. Environ. Qual. 35 (6), 2360–2373.
Srivastava, P., Yadav, A.K., Mishra, B.K., 2015. The effects of microbial fuel cell integration into constructed wetland on the performance of constructed wetland. Bioresour. Technol. 195, 223–230.
Teiter, S., Mander, Ü., 2005. Emission of N_2O, N_2, CH_4, and CO_2 from constructed wetlands for wastewater treatment and from riparian buffer zones. Ecol. Eng. 25 (5), 528–541.
Velvizhi, G., Mohan, S.V., 2012. Electrogenic activity and electron losses under increasing organic load of recalcitrant pharmaceutical wastewater. Int. J. Hydrog. Energy 37 (7), 5969–5978.
Vymazal, J., 2014. Constructed wetlands for treatment of industrial wastewaters: a review. Ecol. Eng. 73, 724–751.
Vymazal, J., Březinová, T., 2015. The use of constructed wetlands for removal of pesticides from agricultural runoff and drainage: a review. Environ. Int. 75, 11–20.
Wang, J.F., Song, X.S., Wang, Y.H., Abayneh, B., Li, Y.H., Yan, D.H., Bai, J.H., 2016. Nitrate removal and bioenergy production in constructed wetland coupled with microbial fuel cell: establishment of electrochemically active bacteria community on anode. Bioresour. Technol. 221, 358–365.
Wu, J., Zhang, J., Jia, W.L., Xie, H.J., Gu, R.R., Li, C., Gao, B.Y., 2009. Impact of COD/N ratio on nitrous oxide emission from microcosm wetlands and their performance in removing nitrogen from wastewater. Bioresour. Technol. 100 (12), 2910–2917.
Wu, S.B., Austin, D., Liu, L., Dong, R.J., 2011. Performance of integrated household constructed wetland for domestic wastewater treatment in rural areas. Ecol. Eng. 37, 948–954.
Wu, H.M., Lin, L., Zhang, J., Guo, W.S., Liang, S., Liu, H., 2016. Purification ability and carbon dioxide flux from surface flow constructed wetlands treating sewage treatment plant effluent. Bioresour. Technol. 219, 768–772.
Wunderlin, P., Lehmann, M.F., Siegrist, H., Tuzson, B., Joss, A., Emmenegger, L., Mohn, J., 2013. Isotope signatures of N_2O in a mixed microbial population system constraints on N_2O producing pathways in wastewater treatment. Environ. Sci. Technol. 47 (3), 1339–1348.
Xu, L., Zhao, Y.Q., Wang, X.D., Yu, W.Z., 2018. Applying multiple bio-cathodes in constructed wetland-microbial fuel cell for promoting energy production and bioelectrical derived nitrification-denitrification process. Chem. Eng. J. 344, 105–113.
Yadav, A.K., 2010. Design and development of novel constructed wetlands cum microbial fuel cell for electricity production and wastewater treatment. Proceedings of 12th International Conference on Wetland Systems for Water Pollution Control (IWA), 4–10th October 2010. Italy, Venice.
Yadav, A.K., Dash, P., Mohanty, A., Abbassi, R., Mishra, B.K., 2012. Performance assessment of innovative constructed wetland-microbial fuel cell for electricity production and dye removal. Ecol. Eng. 47, 126–131.
Yan, C., Zhang, H., Li, B., Wang, D., Zhao, Y.J., Zheng, Z., 2012. Effects of influent C/N ratios on CO_2 and CH_4 emissions from vertical subsurface flow constructed wetlands treating synthetic municipal wastewater. J. Hazard. Mater. 203, 188–194.
Zhang, D., Gersberg, R.M., Keat, T.S., 2009. Constructed wetlands in China. Ecol. Eng. 35, 1367–1378.
Zhang, D., Jinadasa, K.B.S.N., Gersberg, R.M., Liu, Y., Ng, W.J., Keat, T.S., 2014. Application of constructed wetlands for wastewater treatment in developing countries – a review of recent developments (2000−2013). J. Environ. Manag. 141, 116–131.
Zhao, Y.Q., Collum, S., Phelan, M., Goodbody, T., Doherty, L., Hu, Y.S., 2013. Preliminary investigation of constructed wetland incorporating microbial fuel cell: batch and continuous flow trials. Chem. Eng. J. 229, 364–370.